

Active Cancellation of PMSM Torque Ripple Caused by Magnetic Saturation for EPS Applications

Geun-Ho Lee[†]

[†]Dept. of Electrical Eng., The Gyeongnam Provincial Namhae College, Namhae, Korea

Abstract

This paper deals with a control method to reduce the torque ripple of a permanent magnet synchronous motor (PMSM) for electric power steering (EPS) systems. Such an application requires a very low torque ripple in order to maintain a good steering feel. However, because of spatial limitations, it cannot help having a partial saturation in the iron core of the PMSM for an EPS system, and this saturation results in a significant torque ripple. Thus, this paper analyzes the torque ripple caused by the magnetic saturation of a PMSM and proposes a method with respect to inductance measurement to verify the partial saturation. In addition, it is shown that a compensation current is needed in order to minimize the torque ripple when a PMSM is driven in the high torque region. The estimation process of the current and the torque ripple decreased by the current are presented and verified with test results.

Key Words: Electric power steering, Magnetic saturation, Permanent magnet synchronous motor, Torque ripple reduction

I. INTRODUCTION

Electric power steering (EPS) is a system that supplies motor power directly to the steering in order to assist steering torque. Compared to a conventional hydraulic power steering (HPS) system, where an oil pump is driven by the engine, the EPS contributes positively to the environment by improving fuel economy, reducing CO_2 emissions and eliminating oil waste. As a result, HPS is increasingly being replaced by EPS [1], [2].

A permanent magnet synchronous motor (PMSM) has been applied to the performance improvement of EPS. Because PMSMs have many advantages such as high efficiency and high torque per rotor volume, they are especially suitable for automotive applications where space and energy savings are critical.

In the column type EPS system, the PMSM is linked to the steering shaft via a reduction gear, so that the motor vibrations and torque fluctuations are transferred directly through the steering wheel to the hands of the driver. Because of this, only a ripple between one and three percent of rated torque is permitted. There are a lot of technical papers that present motor design and control techniques to reduce cogging torque and torque pulsations [3], [4].

Many active torque ripple cancellation methods [5], [6] have

been suggested. However, high reliability and a simple method are needed in EPS systems.

This paper, on the other hand, shows an estimation method for the compensation current necessary to suppress the torque ripple caused by the magnetic saturation in the PMSM.

Due to the spatial limitations in EPS applications, the magnetic saturation in the stator core is inevitable in the high torque region. This paper analyzes the torque ripple generated through the partial saturation in motors fabricated for EPS systems. Furthermore, the d-axis inductance is measured to prove the saturation with the use of the discrete fourier transform (DFT). The harmonic current distribution, which should be added to the q-axis current to minimize the torque ripple, is calculated by the finite element method (FEM), and the effective method in the PMSM driver is proposed in order to make the harmonic current. In the end, the results are verified by a test.

II. PMSM FOR ELECTRIC POWER STEERING

A. Characteristics of a PMSM for EPS

Fig. 1 indicates a fabricated PMSM for a column type EPS system and the rotor configuration skewed to reduce cogging torque. The specifications of the PMSM are listed in Table I. The cogging torque and total harmonic distortion (THD) of the back-EMF required in the motor are less than 0.02Nm and 0.7% respectively. The torque waveforms are shown in Fig. 2 when the PMSM is driven with a constant q-axis current. In order to measure the torque ripple accurately, the motor

Manuscript received Nov. 17, 2009; revised Feb. 10, 2010

[†]Corresponding Author: motor@namhae.ac.kr
Tel: +82-55-860-5354, Fax: +82-55-860-5351, Namhae college
Dept. of Electrical Eng., The Gyeongnam Provincial Namhae college,
Korea

is driven at 10rpm, and the input current is controlled with a THD that is less than 0.5%. The 6 times torque ripple of the electric frequency goes up as the magnetic torque grows higher. Thus, even if it has good characteristics in the low torque region, the torque ripple generated at the rated torque cannot be neglected.

TABLE I
SPECIFICATIONS OF PMSM

Items	Value
Stator outer diameter	75 mm
Rotor outer diameter	40 mm
Br (@20 ~ 25°C)	1.35 T
Number of poles	6
Rated torque	4 Nm
Rated current	54 Arms
Base and Max. speed	1000, 2000 rpm

B. Inductance Measurement of a PMSM

In this section, an inductance measurement method is presented to demonstrate the magnetic saturation effect of a PMSM. The effect can be observed from the stator winding terminals as a change of inductance. The inductance depends on the input current and the rotor position. The measurement of the inductance is achieved by using a DFT with a high frequency current injection. The equivalent circuit for the vector control of a PMSM is based on a synchronously rotating reference frame, and the mathematical model of the equivalent circuit and torque are given as follows:

$$\begin{bmatrix} V_d \\ V_q \end{bmatrix} = \begin{bmatrix} R_a + pL_d & -\omega L_q \\ \omega L_d & R_a + pL_q \end{bmatrix} \begin{bmatrix} i_d \\ i_q \end{bmatrix} + \begin{bmatrix} 0 \\ \omega\psi_a \end{bmatrix} \begin{bmatrix} i_d \\ i_q \end{bmatrix} \quad (1)$$

$$T = P_n \{ \psi_a i_q + (L_d - L_q) i_d i_q \} \quad (2)$$

where, i_d and i_q are the d and q components of the armature current; v_d and v_q are the d and q components of the terminal voltage; ψ_a is $\sqrt{3/2}\psi_f$; ψ_f is the maximum flux linkage of

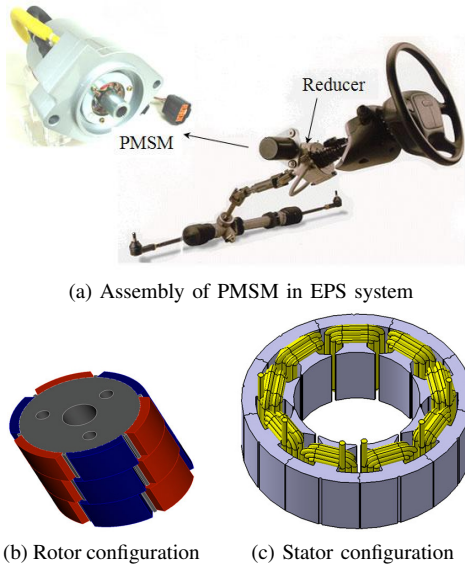


Fig. 1. PMSM fabricated for the column typed EPS.

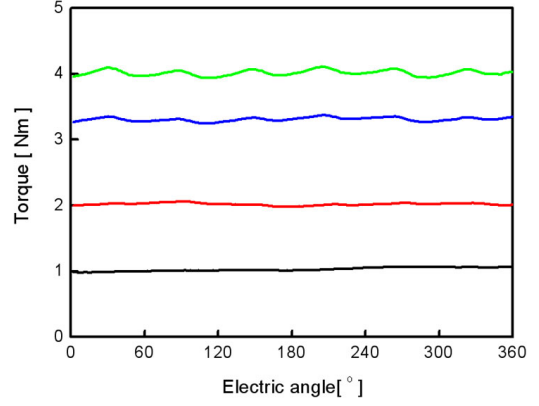


Fig. 2. Torque waveforms measured at 10rpm according to I_q command.

the permanent magnet; R_a is the armature winding resistance; L_d and L_q are the inductance along d- and q-axis; $p = d/dt$; P_n is the number of pole pairs. The saturation phenomenon occurs in all three phases and it can be converted to the orthogonal d-q coordinates oriented toward a desired direction decided by the angle (Θ). A high frequency alternating current is injected into the synchronously rotating frame, and the inductance is measured at each angle when the PMSM is rotating. The d-axis behaves as a resistance and inductance.

$$\frac{V_{dac}(\omega)}{I_{dac}(\omega)} = R + j\omega L_d \quad (3)$$

$$\omega L_d = \text{imag} \left\{ \frac{V_{dac}(\omega)}{I_{dac}(\omega)} \right\} \quad (4)$$

$$X(\omega_o) = \frac{1}{N} \sum_{n=0}^{N-1} x(nT_s) \cdot e^{-j\omega_o nT_s} = a_1 - jb_1. \quad (5)$$

To measure the d-axis inductance at a given angle, the axis is excited with a periodic small signal having the frequency ω_o and sampled N times per period. The value of the commanded voltage and feedback current are measured at the excitation frequency of the small signal by using a DFT. The inductance is calculated from the voltage and current coefficients after one or several periods of small signal excitation.

$$a_1 = \frac{1}{N} \sum_{n=0}^{N-1} x(nT_s) \cdot \cos(\omega_o nT_s) \quad (6a)$$

$$b_1 = \frac{1}{N} \sum_{n=0}^{N-1} x(nT_s) \cdot \sin(\omega_o nT_s) \quad (6b)$$

$$L_d = \frac{1}{\omega_o} \frac{a_{1Vd} \times b_{1Id} - a_{1Id} \times b_{1Vd}}{a_{1Id}^2 + b_{1Id}^2} \quad (7)$$

where, a_{1Id} and a_{1Vd} are the fourier coefficients of current and voltage.

Fig. 3 displays a block diagram of the measurement which has a high frequency current reference, a BPF (Band Pass Filter) and a DFT block in the vector controller. When the motor is running at a low speed, three percent of the rated current with 500Hz is injected, and the I_{de} and V_{de} signals are filtered by a BPF.

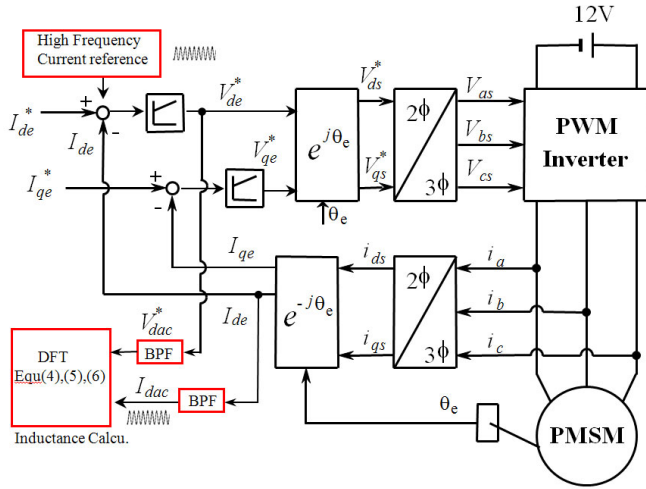


Fig. 3. Inductance measurement block diagram in the vector control.

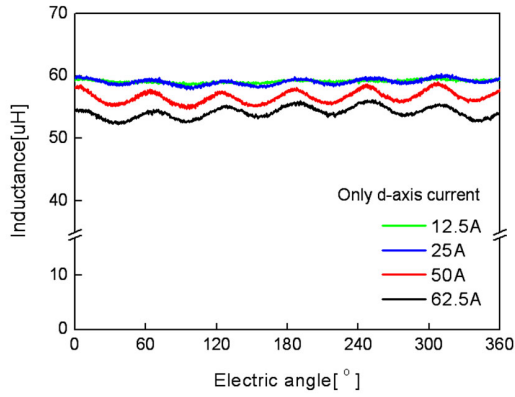


Fig. 4. D-axis inductance according to electric angle.

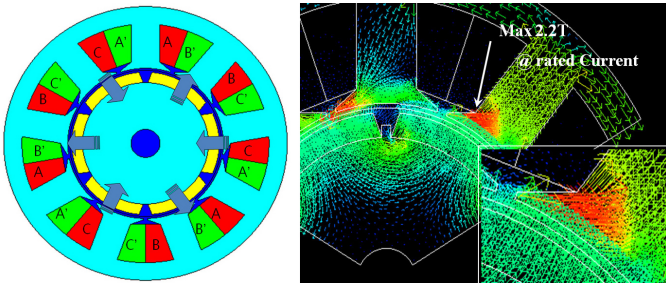


Fig. 5. Flux density distribution at rated current.

The d-axis inductance is decreased according to the d-axis current increase, and it has 6 times the fluctuation of the electric frequency shown in Fig. 4. We find that the partial saturation of the stator teeth makes 6 times the torque ripple of the electric frequency in the PMSM.

III. ACTIVE CANCELLATION CURRENT

In this paper, FEA is used in order to analyze the characteristics of the PMSM and get the waveform of the injection current to reduce the torque pulsation. Nonlinear analysis considers the magnetic saturation of the stator core. Fig. 5 shows the flux density distribution, and the maximum flux density of the stator teeth indicates 2.2T at the rated current.

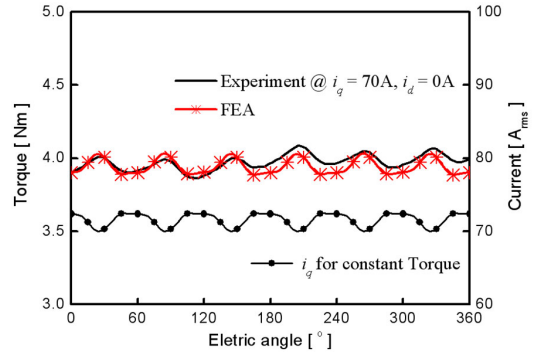


Fig. 6. Torque waveform comparison of analysis and test result.

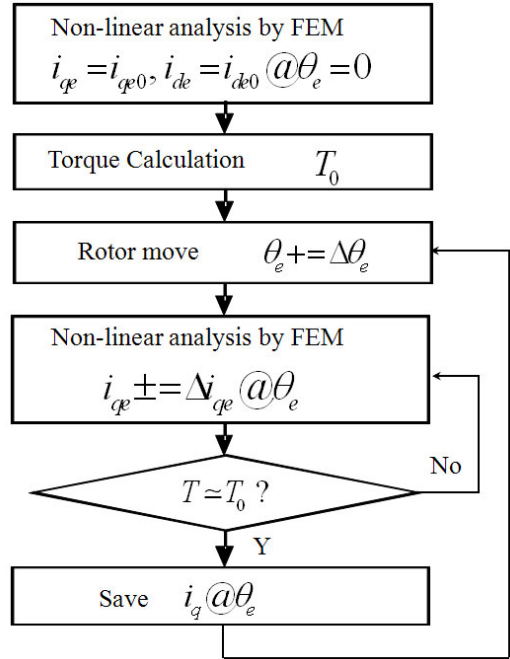


Fig. 7. Flowchart for the estimation of compensation current.

As shown in Fig. 6, the torque characteristics of the PMSM are obtained by FEA, and the analysis results are compared to the experimental results. The results at the rated current are similar to the experimental results. In the test, the PMSM is rotated at a low speed in order to drive the motor with a sinusoidal current. In this paper, the flow chart displayed in Fig. 7 is employed to obtain the q-axis current distribution which minimizes the torque ripple according to the electric angle e . FEA is iterated at each rotor position with a varying I_{qAC} to search for the flat torque waveform.

$$i_q = i_{q0} + i_{qAC} \quad (8)$$

where, i_{q0} is the q component of the armature current for the rated torque; i_{qAC} is the compensation current added to the i_{q0} in order to minimize the torque ripple.

From this method, the compensation current, which can minimize the torque fluctuation, is calculated according to the current angle and it is expressed in Fig. 8. At the rated torque, a 2.5A peak current is added to the q-axis current.

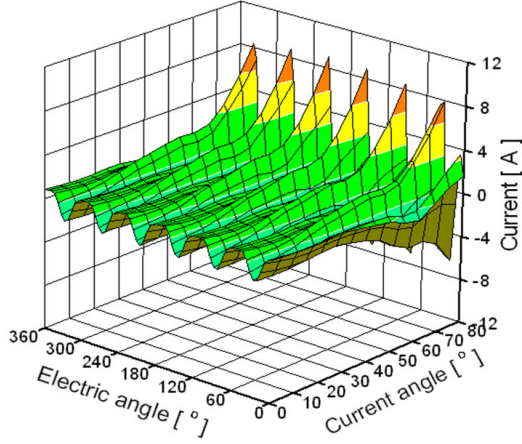


Fig. 8. Compensation current distribution according to current angle.

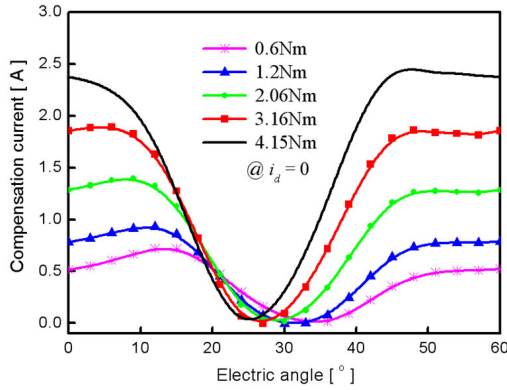


Fig. 9. Compensation current distribution according to a given torque.

IV. STRATEGY FOR THE CANCELLATION OF TORQUE RIPPLE AND TEST RESULTS

The compensation current according to a given torque is obtained as in Fig. 9 while the d-axis current is controlled to zero. As shown in Fig. 10, the harmonics of the compensation current displayed in Fig. 9 consist of the 6th, 12th, 18th and 24th harmonic components according to the q-axis current. Therefore, if the 18th and 24th harmonic components are neglected, the current can be simplified as a function of i_{q0} :

$$i_{qAC} = \sqrt{0.062 + 0.00028i_{q0}^2} \cdot \cos(6\theta_e) + (0.071 + 0.0056i_{q0}) \cdot \cos(12\theta_e). \quad (9)$$

Fig. 11 shows the effective real time compensation strategy to minimize the torque ripple caused by the magnetic saturation in the vector controller. In Table II, the experimental equipment is briefly shown. The most recent digital signal processor, a TMX320F28335 by Texas Instrument, is employed in order to drive the motor. Because of the very low inductance, we chose a 20kHz switching frequency to minimize the high frequency current ripple.

The active cancellation current is calculated and added to the sinusoidal phase current so that the phase current is distorted as in Fig. 12.

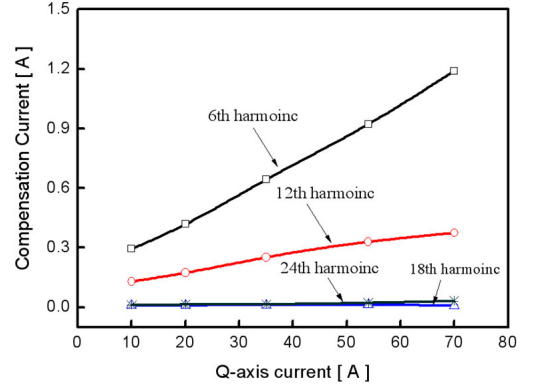


Fig. 10. Harmonic components in the compensation current.

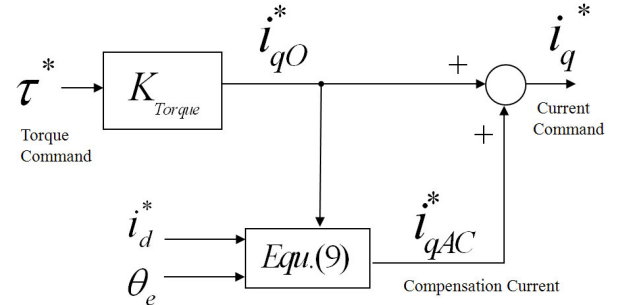


Fig. 11. Compensation strategy in the vector control.

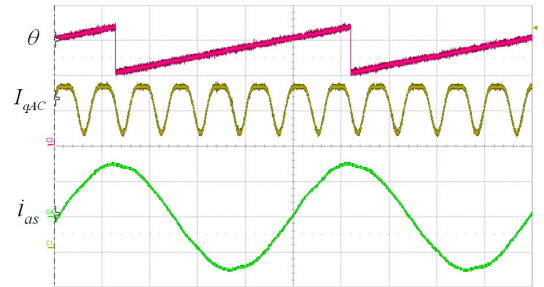
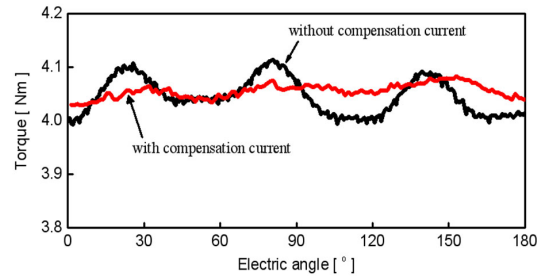
Fig. 12. Active cancellation current and phase current (Θ [5rad/div], I_{qAC} [1A/div], i_{as} [50A/div], X-axis[0.5s/div]).

Fig. 13. Torque waveform at rated current.

From the test results, the 6 times torque harmonic of the electric frequency is decreased to 30% as shown in Fig. 13. By injecting only 2% of the rated current, the torque ripple caused by the partial saturation was effectively suppressed. Fig. 13 shows the testing equipment to measure the torque ripple.

TABLE II
EXPERIMENTAL EQUIPMENT

Items	Value
Switching frequency	20 kHz
DSP	TMX320F28335
Power switch	MOSFET-GWM 220-004
Torque transducer	HBM-T34FN
DC link voltage	12 V

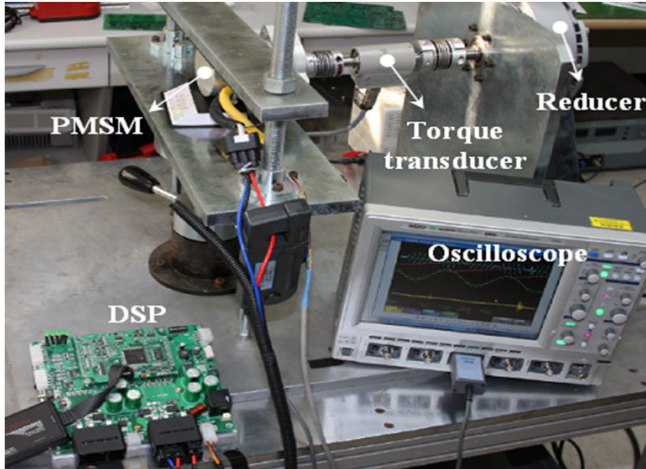


Fig. 14. Testing apparatus for measuring torque ripple.

V. CONCLUSIONS

In this paper, an effective real time inductance measurement method using the DFT was presented to obtain the inductance distribution according to the rotor position. This measurement method was used in order to prove the magnetic saturation of the PMSM. Moreover, the saturation effect was analyzed by a nonlinear analysis, and a simple active cancellation strategy to

minimize the torque ripple at each electric angle was proposed. Finally, the validity of the analysis and compensation method was verified by the test results of a PMSM fabricated for the EPS. With the proposed method, the torque ripple caused by the magnetic saturation could be effectively reduced at the rated torque.

REFERENCES

- [1] Shimizu, Y. and Kawai, T., "Development of electric power steering," *SAE Paper No.910014*, 1991.
- [2] Nakayama, T. and Suda, E., "The present and future of electric power steering," *Int. J. of Vehicle Design*, Vol.15, Nos 3/4/5, pp.243-254, 1994.
- [3] Bianchi, N. and Bolognani, S., "Design techniques for reducing the cogging torque in surface-mounted PM motors," *IEEE Trans. Ind. Applicat.*, Vol.38, No.5, 1259-1265, Sep./Oct. 2002.
- [4] Islam, M. S., Mir, S., Sebastian, T. and Underwood, S., "Design considerations of sinusoidally excited permanent-magnet machines for low-torque-ripple applications," *IEEE Trans. Ind. Applicat.*, Vol.41, No.4, 955-962, Jul./Aug. 2005.
- [5] Mattavelli, P., Tubiana, L. and Zigliotto, M., "Torque-ripple reduction in PM synchronous motor drives using repetitive current control," *IEEE Trans. Power Electron.*, Vol.20, No.6, 1423-1431, Nov. 2005.
- [6] Tinghsu Su, Satomi Hattori, Muneaki Ishida, "Suppression control method for torque vibration of AC motor utilizing repetitive controller with fourier transform," *IEEE Trans. Ind. Applicat.*, Vol.38, No.5, 1316-1325, Sep./Oct. 2002.



Geun-Ho Lee was born in Gyeongnam, Korea, in 1969. He received his B.S. and M.S. in Electrical Engineering from the University of Hanyang, Seoul, Korea, in 1992 and 1994, respectively. He is currently pursuing his Ph.D. in Automotive Engineering from Hanyang University. From 1994 to 2002, he worked with the LG Industrial System where he developed inverter systems for elevators. Since 2002, he has been with the Department of Electrical Engineering, Faculty of Engineering, Namhae College, Gyeongnam Province, where he is currently a Professor. His research interests include the advanced control of electrical machines and power electronics.